

Comparative Analysis of Complexity-Image Quality Trade-offs in Ultrasound Systems for Efficient Hardware Implementation

Zahraa Alzein¹, Ali Ibrahim², Marco Crocco³, Marco Merlanti³, Daniele D. Caviglia¹

¹DITEN Department, University of Genova

Via All 'Opera Pia 11a, Genova, Italy

zahraa.alzein@edu.unige.it ali.ibrahim@liu.edu.lb

² EEE Department, Lebanese International University (LIU)

Mouseitbeh, Beirut, Lebanon

daniele.caviglia@unige.it

³Esaote S.p.A

marco.crocco@esaote.com marco.merlanti@esaote.com

Abstract - This paper presents a comprehensive investigation into the hardware design considerations for focused transmit ultrasound systems, focusing on the trade-off between image quality and computational efficiency. Five distinct channel configurations were simulated, and the results were validated with real-time images acquired from an ultrasound scanner at two different center frequencies. Image quality was assessed using resolution measurements employing both axial and lateral metrics for both simulated and real images. The findings reveal that lower channel count configurations can be viable for balancing portability, cost-effectiveness, and acceptable image quality for specific diagnostic applications. . This study provides valuable insights into the optimal hardware design for linear array ultrasound systems, demonstrating that higher frequencies can improve image quality even with fewer channels, thereby reducing computational costs and hardware complexity.

Keywords: ultrasound system, linear array, image quality, computational cost

1. Introduction

Ultrasound is a safe and non-invasive diagnostic modality that employs advanced imaging techniques considered the preferred method for examining various diseases [1]. B-mode ultrasound (US) imaging is one of the most frequently used diagnostic tools in a wide range of clinical applications [2]. B-mode images are available in real-time offering minimal health risks to patients with relatively low scan costs compared to other imaging modalities.

Image quality is a critical metric in healthcare imaging systems. However, achieving high image quality often results in high costs, large sizes, and significant power consumption and requires high channel numbers in the entire design of the ultrasound machine. In the context of a high number of channels, Kidav et al. [3] proposed 128-channel transceiver hardware, and Assef et al. [4] introduced a 128-channel FPGA-based ultrasound imaging beamformer, offering enhanced control and programmability for signal processing. In handheld ultrasound imaging, Roa et al. [5] developed a low-power 16-channel Analog Front-End, reducing power requirements and extending battery life. Fournelle et al. [6] presented a portable, low-cost ultrasound research system that allows access to pre-beamformed channel data from 32 channels, showing promising imaging performance for research and clinical settings. Low-channel ultrasound systems have advantages like reduced power consumption, longer battery life, and cost-effectiveness for point-of-care applications. However, they may have limitations in spatial resolution and image quality. Researchers have explored techniques like synthetic aperture imaging and adaptive beamforming to enhance image quality in low-channel systems [7][8]. However, a drawback of these approaches is the computational cost associated with these methods, which can significantly increase the system's processing time and resource requirements.

From this perspective, this study aimed to evaluate the trade-offs between image quality and computational cost to give insights into the adequate hardware design for a linear array ultrasound system utilized in B-mode imaging. The main contributions of this study are summarized as follows:

- Implementing a focused transmit linear array ultrasound system for simulation: Field II [10-11] was used to generate B-mode images with five different channel configurations.
- Generate real-time B-mode images of a cyst phantom with the same channel configurations and same center frequencies using a MyLab9 ultrasound scanner and a linear array L3-11 transducer.
- Provide a quantitative analysis of the ultrasound system size by evaluating axial and lateral resolution and complexity and then illustrate the related results.

2. Materials and Methods

This study aims to analyse the impact of channel count on image quality and computational cost in focused transmit ultrasound systems. To achieve this, the planned scenario consists of designing a simulation system and then validating the simulation with real images. To this end, two different experiments have been performed: 1) the first using simulated data generated from Field II [9, 10] simulator considering different channel configurations and center frequencies, and 2) the second based on real-time B-mode images of a cyst phantom and evaluated using an ultrasound scanner with the same channel configurations and center frequencies as the ones used in the simulation. The channel count ranges from 32 to 192, considering both small-scale and large-scale ultrasound systems. Two distinct frequency settings i.e. high resolution and high penetration are to be used to adjust the center frequency (f_0) of the transmitted signal.

To ensure alignment with the generated real-time B-mode images, the frequencies in the simulated and real images were adjusted to 5 MHz and 8.33 MHz, based on the capabilities of the transducer used. In this paper, image quality for both simulated and real images is evaluated through quantitative analysis of axial and lateral resolution at -6 dB at two focal points, 50 mm, and 100 mm, and by the ultrasound scanner for experimental images. However, the computational complexity is assessed by measuring the processing time and the number of floating-point operations required to generate the B-mode image with multi-scatterers located at different depths.

2.1. Simulation Setup

The linear-array ultrasound system used for the simulation is shown in Fig 1. The system aims to produce B-mode images using five different channel configurations: 32, 64, 96, 128, and 192, where all channels are used in reception. A linear array transducer was modelled in MATLAB using a Field II simulator [9,10]. The transducer comprises 192 elements with a kerf of 30 μm and pitch equal to λ . The elevation focus is fixed at 40 mm. The number of channels was then adjusted to different values, and during transmission, the transducer generated a 2-cycle sinusoidal burst with a Hann window shaping the pulse envelope. The transmitted signal's center frequency (f_0) was adjusted to 5 MHz and 8.33 MHz. Then, Delay and Sum Beamforming (DAS) [11,12], the standard technique used for image reconstruction in ultrasound, is implemented for transmission and reception. Each transducer element in the array has a specific associated time delay calculated based on the distance between each element and the focal point. The delayed signals from each transducer were then summed, resulting in a focused ultrasound beam. A dynamic apodization with a F-number equal to 0.7 using the Blackman harries window is used to apply weighting coefficients across the transmit signal and received RF data to reduce the effects of side lobes.

During reception, the transducers switch to detecting echoes applying time delays again to synchronize signals from various depths. A sampling rate equal to thirty times the central frequency is applied. The beamformed signals undergo envelope detection using the Hilbert transform followed by dynamic logarithmic compression. Finally, the resulting signals create and display the 2-D B-mode image over a dynamic range of 60 dB.

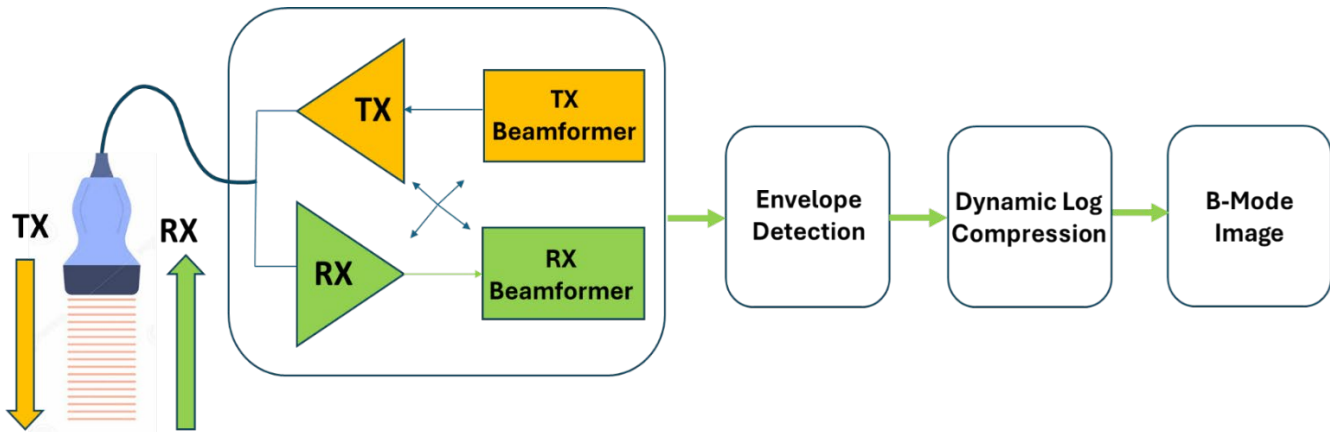


Fig.1: Block Diagram of Linear Array Ultrasound System

2.2 B-Mode Image Acquisition with CIRS Phantom

Real-time B-mode images of the CIRS Model 040GSE multi-tissue phantom [13] were acquired using a MyLab9 ultrasound imaging system (Esaote, Genova, Italy) equipped with a linear array L3-11 transducer. The L3-11 transducer is a 192-element probe with a central frequency of 5.8 MHz. The imaging parameters were set to a region of interest (ROI) with a depth of 176 mm and a transmission focal depth of 40 mm. B-mode images were acquired at two distinct frequencies, 5 MHz and 8.33 MHz, using identical channel configurations as those employed in the simulation. The data acquisition sampling rate was set to 50 MHz.

3. Results and Discussion:

3.1. Simulated PSFs at Different Depths

The PSF lateral profiles with several point scatterers, placed side by side at different depths (from 0 to 150 mm with a 5 mm step) along the $x = -10$ mm, $x = 0$ mm, and $x = 10$ mm axial directions, as represented in Figure 2, reveal that a higher center frequency (8.33 MHz) leads to demonstrably enhanced lateral resolution, evidenced by narrower PSFs and a reduction in side lobes compared to a lower center frequency (5 MHz), even with low channel counts such as 64 and 96. We can still achieve clear scatterers at shallower depths, i.e., 40 mm and 50 mm. This can be attributed to the improved spatial resolution inherent in higher frequencies, which allows for tighter focusing and reduced signal spread. However, when using 5 MHz, the scatterers are well seen even at deeper depths, i.e., 100 mm and beyond. This implies a potential trade-off between lateral resolution and penetration depth, where lower frequencies might offer advantages for deeper imaging applications.

From a quantitative point of view, the -6 dB axial resolution does not exhibit a noticeable change with varying channel numbers, remaining between ~ 0.32 mm and ~ 0.37 mm for both 5 MHz and 8.33 MHz frequencies as we increase the number of channels from 32 to 192. However, the main impact is on lateral resolution, as quantitatively illustrated in Figure 3, where the lateral resolution for two focal points (50 mm and 100 mm) is measured using FWHM. Notably, contrast resolution appears to benefit from higher frequencies irrespective of the number of channels employed, particularly at shallower depths. This offers advantages in applications that do not require high penetration depths, such as superficial applications, emergency applications, and point-of-care settings. This suggests that the frequency-dependent improvement in contrast may be a dominant factor, potentially due to increased signal-to-noise ratio at higher frequencies.

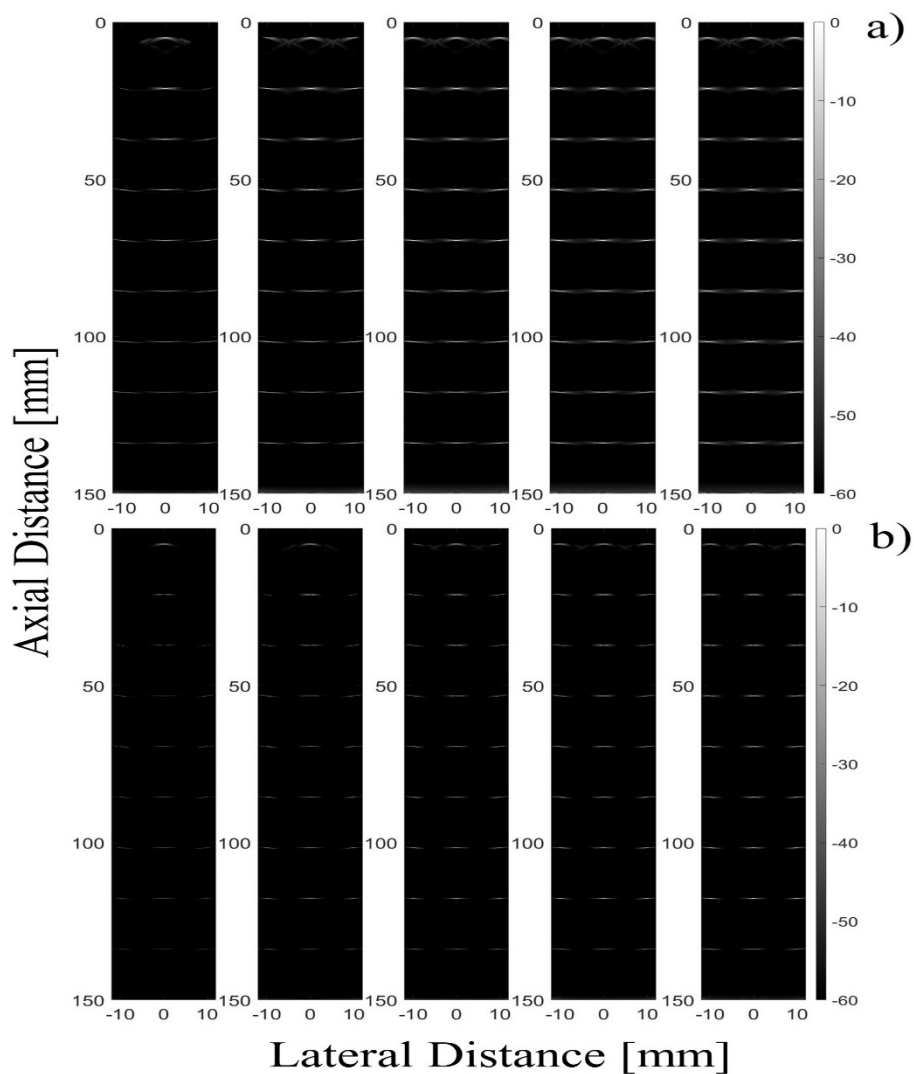


Fig. 2 : PSFs obtained by using different channel configurations (32, 64, 96, 128, 192) at a frequency of a) 5 MHz and b) 8.33 MHz. The images are arranged from left to right in ascending order of channel count. Images are displayed over a 60 dB dynamic range

3.2. Cyst phantom Images

Real-time B-mode images acquired by the ultrasound scanner presented in Figure 4 showcase a cyst phantom imaged at two distinct frequencies (5 MHz and 8.33 MHz). Consistent with the PSF analysis, the 8.33 MHz frequency yields high-resolution B-mode images at shallower depths. These images exhibit detailed and uniform cyst structures (Fig. 4). Conversely, the 5 MHz images acquired at this depth display a slight decrease in resolution compared to the 8.33 MHz

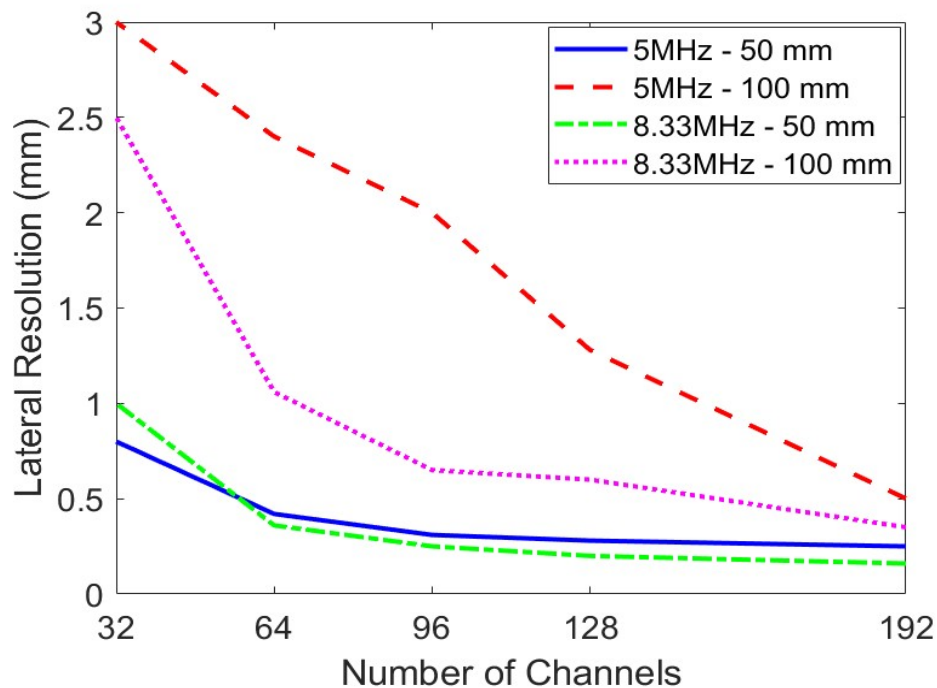


Fig.3 : Lateral Resolution Using 5MHz and 8.33MHz for Different Channel Configurations for Simulated Images

images. However, at greater depths, the cyst remains visible in the 5 MHz images, highlighting the effectiveness of lower frequencies in penetrating deeper tissues.

The number of channels employed in the ultrasound scanner significantly influences image clarity. As the number of channels increases, visualization and uniformity of cyst structures improve. The quantitative measurements on the impact of channel configuration on lateral resolution are presented in Figure 5, demonstrating the same trend consistent with the simulation results. This reinforces the notion that the number of channels primarily affects lateral resolution, with minimal influence on axial resolution. Axial resolution changes only slightly, ranging from ~0.53 mm to ~0.67 mm as the number of channels increases from 32 to 192. The highest lateral resolution is achieved with the 192-channel configuration at 8.33 MHz and a shallower depth (50 mm), aligning with the findings from the simulations. Furthermore, utilizing 8.33 MHz still allows for acceptable lateral resolution even with a lower number of channels (e.g., 64 channels) at shallower depths, i.e., 50 mm.

3.3 Computational Complexity

The computational load associated with B-mode image generation was evaluated using a CPU with the following specifications: 12th Gen Intel(R) Core (TM) i9-12900K 3.20 GHz, 16.0 GB RAM (Table I). The results demonstrate a significant increase in execution time and floating-point operations (FLOPs) for configurations with a higher channel count, considering that the same imaging grid is used for all channels. As the number of channels decreases, processing time and FLOPs decrease significantly with the 192-channel configuration exhibiting the highest computational load. Furthermore, employing many channels necessitates a higher memory capacity and more hardware resources. For example, on Field-Programmable Gate Array (FPGA) implementations, more pulser and front-end boards are required to manage high channel

counts. Conversely, lower channel configurations (e.g., 64 channels) require fewer resources, allowing for a more portable and cost-effective ultrasound scanner design suitable for emergency applications.

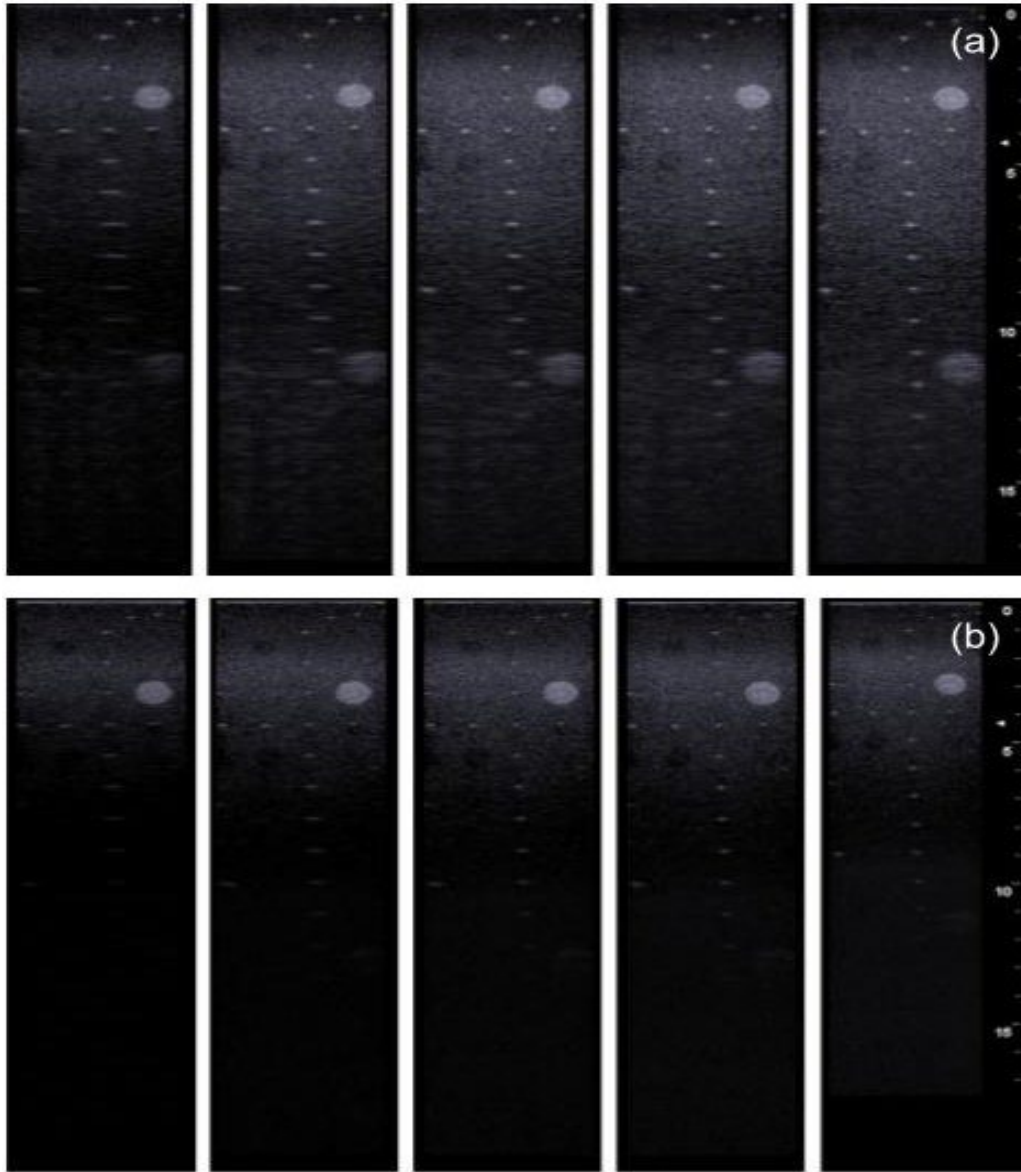


Fig.4: B-mode Images of Cyst phantom acquired using different channel configurations (32, 64, 96, 128, 192) at a frequency of a) 5 MHz and b) 8.33 MHz the images are arranged from left to right in ascending order of channel count.

Notably, a remarkable reduction of over 90% in processing time and a 74.98% reduction in FLOPs can be achieved with a 64-channel configuration, while still maintaining acceptable image quality at shallower depths, incomparable to the 192-channel configuration that achieves the highest image quality.

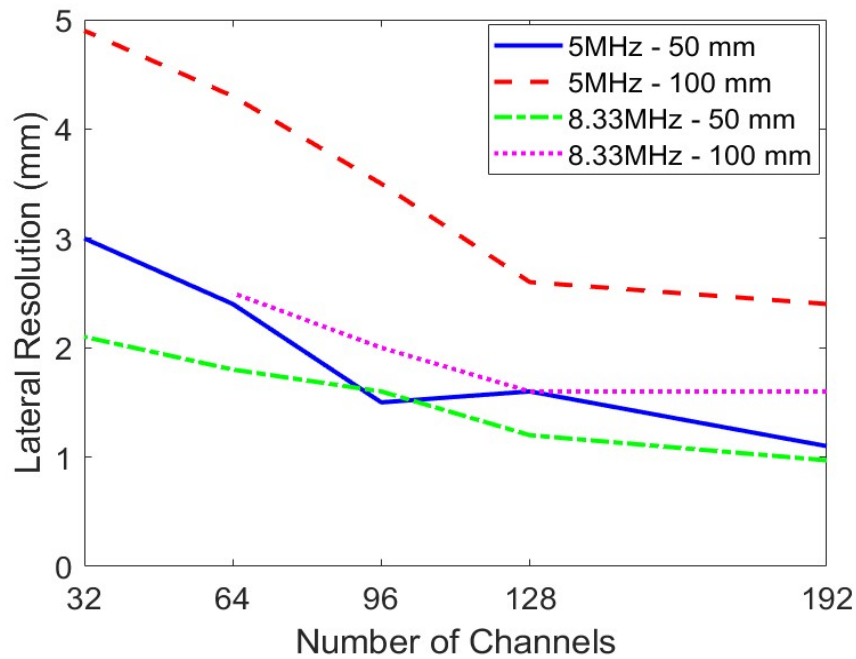


Fig.5 : Lateral Resolution at 50mm and 100 mm Using 5MHZ and 8.33MHZ for Different Channel Configurations for Images Acquired by the Ultrasound Scanner

We can further consider employing dynamic apodization, where each focal point (FP) requires an apodization window. For example, let's assume we have 500 FPs. Each apodization window necessitates 192 distinct values, corresponding to the number of transducer elements. Therefore, for a 12-bit representation, the total size of the required coefficients is approximately 221 Mbits ($12 * 192 * 192 * 500$). These coefficients must be calculated on the fly and stored in Block RAM (BRAM) memories [14], which adds more expenses to the design of the machine and incurs additional costs. However, it is worth noting that this size can be reduced to approximately 24 Mbits when using a 64-channel configuration, providing a more efficient use of resources and potentially lowering costs.

Table I: Execution Time and FLOPS for Different Channel Configurations

Number of channels	Processing time (seconds)	FLOPS ($\times 10^8$)
192	119.24	9.75
128	53.80	7.93
96	29.42	5.49
64	13.78	2.44
32	3.86	0.61

4. Conclusion:

The choice of hardware design for an ultrasound system involves a trade-off between image quality, complexity, and cost. It is essential to achieve good image quality while keeping costs and complexity at acceptable levels. While this study

primarily focused on resolution measurements, future investigations should incorporate additional key image quality metrics such as signal-to-noise ratio (SNR) and contrast-to-noise ratio (CNR). These metrics can be evaluated through the simulation of synthetic phantoms and further validated with experimental analysis using an established CIRS model. Building on the observed trade-off between computational cost and image quality, this study demonstrates that utilizing a lower channel count configuration can be a viable approach for achieving a balance between portability, cost-effectiveness, and acceptable image quality. This approach is particularly effective when employing a higher center frequency since higher frequencies offer improved image quality even with fewer channels. However, the optimal channel count will depend on the specific application requirements and the desired level of image quality. Future research will investigate advanced signal processing techniques, leveraging the quantitative analysis presented in this paper for comparisons. Additionally, exploring novel hardware architectures holds promise for further advancing the capabilities of focused transmit ultrasound systems, enabling them to achieve high image quality with a reduced number of channels. This ongoing research aims to enhance the performance and cost-effectiveness of ultrasound systems paving the way for improved diagnostic capabilities in various clinical applications.

References

- [1] Genc, Alicja, Ryk, Małgorzata, Suwała, Magdalena, Żurakowska, Tatiana and Kosiak, Wojciech. "Ultrasound imaging in the general practitioner's office – a literature review" *Journal of Ultrasonography*, vol.16, no.64, 2016, pp.78-86.
- [2] Guofang Xiao, M. Brady, J. A. Noble, and Yongyue Zhang, "Segmentation of ultrasound B-mode images with intensity inhomogeneity correction," in *IEEE Transactions on Medical Imaging*, vol. 21, no. 1, pp. 48-57, Jan. 2002.
- [3] Kidav, J., Pillai, P. M., V, D., & G, S. S. (2021). Design of a 128-channel transceiver hardware for medical ultrasound imaging systems. *IET Circuits, Devices and Systems*, 16(1), 92-104. <https://doi.org/10.1049/cds2.12087>
- [4] A. A. Assef, J. M. Maia, F. K. Schneider, E. T. Costa and V. L. S. N. Button, "Design of a 128-channel FPGA-based ultrasound imaging beamformer for research activities," *2012 IEEE International Ultrasonics Symposium*, Dresden, Germany, 2012, pp. 635-638, doi: 10.1109/ULTSYM.2012.0158
- [5] E. Roa, K. Beumer, and M. Chirala, "A 16-channel 38.6 mW/ch fully integrated Analog Front-End for handheld Ultrasound imaging," *2014 IEEE Biomedical Circuits and Systems Conference (BioCAS) Proceedings*, Lausanne, Switzerland, 2014, pp. 647-650.
- [6] M. Fournelle, T. Grüm, D. Speicher, S. Weber and S. Tretbar, "Portable low-cost 32-channel ultrasound research system," *2020 IEEE International Ultrasonics Symposium (IUS)*, Las Vegas, NV, USA, 2020, pp. 1-3,
- [7] Rostamikhanghahi H, Sakhaei SM. Synthetic Aperture Ultrasound Imaging through Adaptive Integrated Transmitting-Receiving Beamformer. *Ultrason Imaging*. 2023 May;45(3):101-118.
- [8] S. Dange, "Synthetic Aperture Ultrasound Imaging a Review, 2020 IEEE 4th Conference on Information & Communication Technology (CICT), Chennai, India, 2020, pp. 1-6,
- [9] J.A. Jensen: Field: A Program for Simulating Ultrasound Systems, Paper presented at the 10th Nordic-Baltic Conference on Biomedical Imaging Published in *Medical & Biological Engineering & Computing*, pp. 351-353, Volume 34, Supplement 1, Part 1, 1996.
- [10] J.A. Jensen and N. B. Svendsen: Calculation of pressure fields from arbitrarily shaped, apodized, and excited ultrasound transducers, *IEEE Trans. Ultrason., Ferroelec., Freq. Contr.*, 39, pp. 262-267, 1992
- [11] Soufiane Dangoury, Mohammed Sadik, Abdelhakim Alali, and Saad Abouzahir. 2020. Ultrasound imaging: Beamforming Techniques. *Proceedings of the 2nd International Conference on Advanced Technologies for Humanity (2020)*
- [12] Z. Wang, J. Li, and R. Wu, "Time-delay- and time-reversal-based robust Capon beamformers for ultrasound imaging," *IEEE Transactions on Medical Imaging*, vol. 24, no. 10, pp. 1308–1322, 2005.
- [13] <https://www.cirsinc.com/products/ultrasound/zerdine-hydrogel/multi-purpose-multi-tisse-ultrasound-phantom/>
- [14] W. Heckel, B. Maaref and N. Hassen, "Evaluation of transmit/receive apodization scheme for hardware implementation used in B-mode ultrasound imaging," *2020 17th International Multi-Conference on Systems, Signals & Devices (SSD)*, Mon astir, Tunisia, 2020, pp. 808-813, doi: 10.1109/SSD49366.2020.9364236.